Lignin Peroxidases Can Also Oxidize Manganese†

Aditya Khindaria, David P. Barr, and Steven D. Aust*

Biotechnology Center, Utah State University, Logan, Utah 84322-4705

Received December 29, 1994; Revised Manuscript Received March 27, 1995[⊗]

ABSTRACT: The peroxidase isozymes secreted by the white rot fungus *Phanerochaete chrysosporium* include lignin peroxidases and manganese-dependent peroxidases. The major isozymes, called lignin peroxidases, are thought to oxidize chemicals directly. The manganese-dependent peroxidases (H3, H4, H5, and H9) are relatively minor, making up only a fraction of the total peroxidase protein. However, we have found that lignin peroxidases will also catalyze the H_2O_2-dependent oxidation of Mn^{2+} to Mn^{3+}. We have used lignin peroxidase isozyme H2 (LiPH2) to characterize the manganese peroxidase activity of lignin peroxidases. Transient state kinetic studies were used to obtain a second-order rate constant of 4.2×10^4 M^{-1} s^{-1} for the reaction of LiPH2-compound I with free or chelated Mn^{2+} at pH 6.0. This reaction was too fast to monitor at pH 4.5. Only chelated Mn^{2+} could reduce LiPH2-compound II to ferric enzyme. The Mn^{2+}−chelate (oxalate) first bound LiPH2-compound II with a K_d of $(1.5 \pm 0.3) \times 10^{-5}$ M and then reduced LiPH2-compound II to ferric enzyme with a first order rate constant of 215 ± 6 s^{-1}. Steady-state kinetic studies on LiPH2 were performed by directly monitoring the formation of Mn^{3+}−oxalate. These results show that oxidation of Mn^{2+} by a lignin peroxidase does not occur through free radical mediation as proposed previously [Popp et al. (1990) *Biochemistry 29,* 10475−10480). Electron spin resonance and oxygen evolution studies also indicate that Mn^{2+} is directly oxidized by LiPH2. In addition, veratryl alcohol oxidation by LiPH2 was inhibited in the presence of Mn^{2+}, suggesting that both Mn^{2+} and veratryl alcohol are substrates for LiPH2.

Lignin peroxidases and manganese-dependent peroxidases are partly responsible for lignin and xenobiotic degradation by the white rot fungus *Phanerochaete chrysosporium* (Kirk & Farrell, 1987; Barr & Aust, 1994). Lignin peroxidases (isozymes H1, H2, H6, H7, H8, and H10) oxidize a variety of organic substrates (Tien, 1987). Manganese peroxidases (isozymes H3, H4, H5 and H9) on the other hand, oxidize Mn^{2+} to Mn^{3+} which acts as a diffusable oxidant to oxidize a variety of organic molecules indirectly (Wariishi et al., 1989; Glenn et al., 1986). Electrochemical studies have shown that several physiologically relevant Mn^{3+}−chelates can oxidize lignin model compounds (Cui & Dolphin, 1990).

Manganese levels in wood can reach concentrations of up to 22 mM (Young & Guinn, 1966). Thus, manganese may play an important role in biodegradation of lignin by *P. chrysosporium*, as a mediator or in other roles. However, the manganese-dependent peroxidases only make up a small proportion of the total peroxidases (~30%; based on protein) under our culture conditions (Tuisel et al., 1990). Popp et al. (1990) have suggested that lignin peroxidases can also oxidize manganese but by an indirect mechanism requiring veratryl alcohol (VA)[1] and oxalate. We discovered that Mn^{2+} inhibits the VA oxidase activity of lignin peroxidases. This led us to believe that lignin peroxidases may be involved in the direct oxidation of Mn^{2+}.

In the present study, we have characterized the reactions of LiPH2 with free and chelated manganese. Pre-steady-state techniques were used to study the reaction between Mn^{2+} and LiPH2-compounds I and II. While free or chelated manganese were substrates for LiPH2-compound I, only chelated Mn^{2+} could reduce LiPH2-compound II to the ferric enzyme. Steady-state kinetic data, along with ESR and oxygen evolution studies, are provided as evidence for the direct oxidation of Mn^{2+} by LiPH2. This conclusion is also supported by Mn^{2+}-dependent inhibition of VA oxidation by LiPH2.

MATERIALS AND METHODS

Hydrogen peroxide was purchased from Sigma Chemical Co. (St. Louis, MO). Superoxide dismutase, VA, and manganese sulfate were purchased from Aldrich Chemical Co. (Milwaukee, WI). Sodium oxalate, succinic acid and sodium succinate were purchased from Mallinckrodt (Paris, KY). All chemicals were reagent grade and were used as purchased. Sodium succinate buffer was prepared using purified water (Barnstead NANOpure II system; specific resistance 18.0 MΩ cm^{-1}).

Enzyme Production and Purification. The culture conditions used to produce lignin peroxidases and their purification and activity assay were as described previously (Tuisel et al., 1990). Pure lignin peroxidase isozyme H2 (p*I* 4.4) was used throughout this study. The purity of LiPH2 was determined by the analytical isoelectric focusing technique. Isoelectric focusing was done in a 5.5% polyacrylamide gel using a p*I* gradient of 3−10 (Bio-Lyte 3−10, BioRad). The gel was prefocused immediately prior to use. A maximum of 15 μg of protein was applied per well, and the gel was run at 25 W with a voltage limit of 2500 V for 3 h. Following electrophoresis, the gel was fixed for 45 min and

† This research was supported by NIEHS Superfund Basic Research and Training Grant ESO4922.

* To whom correspondence should be addressed. Telephone: (801) 797-2730. FAX: (801) 797-2755. E-mail: sdaust@cc.usu.edu.

⊗ Abstract published in *Advance ACS Abstracts,* June 1, 1995.

[1] Abbreviations: LiPH2, lignin peroxidase isozyme H2; ESR, electron spin resonance; VA, veratryl alcohol; SOD, superoxide dismutase.

0006-2960/95/0434-7773$09.00/0 © 1995 American Chemical Society

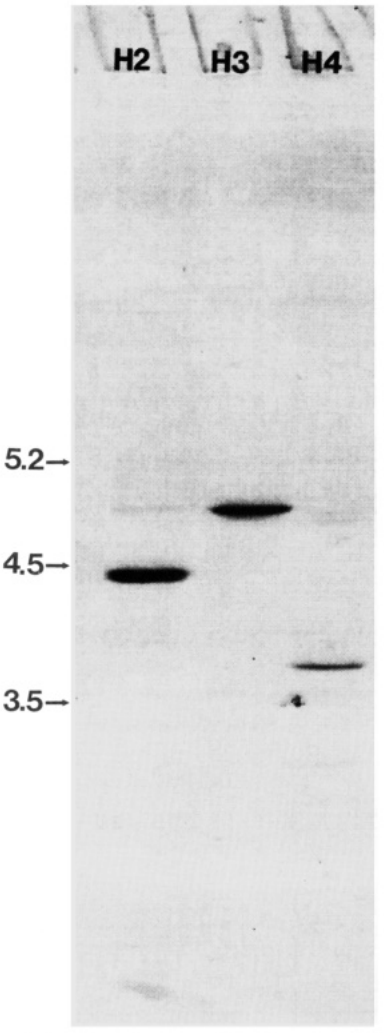

FIGURE 1: Analysis of lignin peroxidase isozyme H2 and manganese peroxidase isozymes H3 and H4 by isoelectric focusing. The isozymes applied to the lanes are identified at the top of the Coomassie blue stained gel. Numbers to the left of the gels indicate pH (as determined by the p*I* of standard proteins). The p*I* of lignin peroxidase isozyme H2 was determined to be 4.4 from this gel. The detailed experimental procedure is given under Materials and Methods.

stained using Coomassie brilliant blue R-250 and destained in 40% ethanol, 10% glacial acetic acid. The p*I* of 4.4 was determined for LiPH2 from the isoelectric focusing gel (Figure 1). This value is consistent with the previously determined p*I* for LiPH2 (Farrell et al., 1989). The analysis of the gel also showed that the LiPH2 used in this study was pure (99%) and was not contaminated with manganese-dependent peroxidases.

Transient State Kinetic Studies. Reduction of compound I to compound II by Mn^{2+} was monitored at 417 nm, the isosbestic wavelength between the resting ferric enzyme and compound II. Reduction of compound II to ferric enzyme was monitored at 397 nm, the isosbestic wavelength between compounds I and II. All reactions were performed at 25 °C.

Pre-steady-state kinetic experiments with compounds I and II were performed under single-turnover, pseudo-first-order conditions. For studies with compound I, the ferric enzyme was first mixed with 1 equiv of H_2O_2 for 1.5 s to allow for complete formation of compound I. It was then reacted with Mn^{2+} to obtain the rate constant for reaction of Mn^{2+} with compound I. Rate constants for the reaction of compound II were determined using compound II generated by the one-electron reduction of compound I by ferrocyanide. In this case, the enzyme and 1 equiv of ferrocyanide were mixed with 1 equiv of H_2O_2 for 2 s to allow for the complete formation of compound II. Compound II so generated was reacted with various concentrations of Mn^{2+}−oxalate complex.

The three-syringe stopped-flow apparatus used for transient-state studies was purchased from KinTek Instruments (State College, PA). Operation and data collection were as described previously (Kuan et al., 1993).

Steady-State Kinetics. The initial velocity of Mn^{2+} oxidation was monitored at 270 nm, the absorbance maximum for Mn^{3+}−oxalate. The amount of Mn^{3+} produced was calculated using an extinction coefficient of 5500 M^{-1} cm^{-1} for Mn^{3+}−oxalate. This extinction coefficient was determined as described previously (Kuan et al., 1993) except that the Mn^{2+} contamination in Mn^{3+} solutions was quantitated using ESR spectrometry. Steady-state kinetic data were obtained with limiting H_2O_2 as higher concentrations of H_2O_2 led to the reaction of H_2O_2 with Mn^{3+}, leading to O_2 evolution. Further details of experiments are provided in the figure legends.

Veratryl alcohol oxidase activity of LiPH2 was determined by following the formation of veratryl aldehyde at 310 nm (Tuisel et al., 1990). For the inhibition studies of VA oxidase activity of LiPH2 by Mn^{2+}−oxalate, the increase in absorbance at 310 nm due to Mn^{3+}−oxalate was subtracted.

ESR Experiments. A Bruker ECS-106 spectrometer operating at 9.8 GHz with a 50 kHz modulation frequency was used for all ESR recordings. Further details of these experiments are given in the figure legends. Noise was filtered from spectra by a Fourier transformation method using the ECS-106 ESR software.

Oxygen Evolution Studies. Oxygen evolution was measured using a Gilson oxygraph monitor equipped with a 1.8 mL reaction chamber, maintained at 25 °C, and a Clark-type oxygen-sensitive electrode. Typical reaction mixtures contained 0.38 μM LiPH2, 100 μM $MnSO_4$, 0.5 mM oxalate (where mentioned), 2 mM VA (where mentioned), and varying amounts of H_2O_2 in 20 mM succinate buffer, pH 4.5.

Simulation of Steady-State Data. Computer simulation of steady-state data using rate constants obtained from pre-steady-state studies was performed with the kinetic simulation program KINSIM (Barshop et al., 1983), provided by Carl Frieden and Bruce Barshop (Washington University, St. Louis, MO).

RESULTS

Reduction of Compound I by Mn^{2+}. At pH 4.5, the physiological pH of the fungus, the reaction of LiPH2-compound I with Mn^{2+} was too rapid to observe at Mn^{2+} concentrations above 10 μM (10 times that of the enzyme concentration to ensure pseudo-first-order kinetics). When the pH was increased to 6.0 in phosphate buffer, the Mn^{2+}-dependent conversion of compound I to II was slow enough to record. The reduction of compound I of LiPH2 by Mn^{2+} at pH 6.0 is shown in Figure 2 (inset). A linear relationship between k_{obs} and Mn^{2+} concentration was observed (Figure 2). A second-order rate constant of 4.2×10^4 M^{-1} s^{-1} was

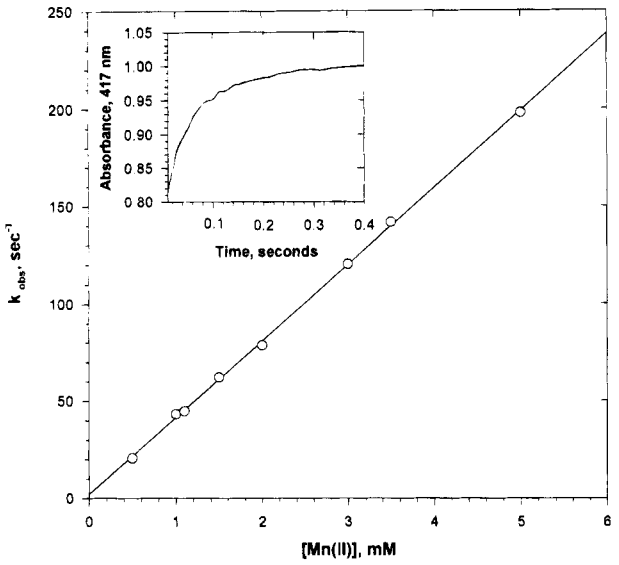

FIGURE 2: Reduction of lignin peroxidase compound I to compound II by Mn^{2+} at pH 6.0. One equivalent of H_2O_2 (1 μM) was mixed with lignin peroxidase (1 μM) for 1.5 s to allow for complete formation of compound I. This was subsequently mixed with varying concentrations of Mn^{2+} in 20 mM phosphate buffer, pH 6.0. The k_{obs} values were obtained from fitting the data for the increase in absorbance at 417 nm. The inset shows the actual stopped-flow trace for the increase in absorbance at 417 nm, corresponding to reduction of compound I to II by 3.5 mM Mn^{2+}.

calculated from the slope. The same rate constant was obtained at pH 3.0 (data not shown). These results were obtained irrespective of whether free or chelated Mn^{2+} was used as a substrate.

Reduction of Compound II by Chelated Mn^{2+}. It has been reported that only chelated Mn^{2+} is a substrate for manganese-dependent peroxidase compound II (Kuan et al., 1993). Therefore, we investigated if this could also be the case for LiPH2-compound II. In 20 mM succinate buffer, Mn^{2+} could not reduce compound II to resting enzyme. The binding constant for chelation of Mn^{2+} by succinate suggested that at the concentration of succinate used Mn^{2+} was present primarily as free manganese (hexaaquo) ion. When oxalate was used as a chelator, Mn^{2+}−oxalate reduced compound II to resting enzyme (Figure 3, inset). This reaction was slow enough to monitor at pH 4.5. At the concentration of oxalate used, Mn^{2+} is predominantly chelated by one oxalate ligand. This indicated that only chelated Mn^{2+} is able to reduce compound II to ferric enzyme. The plot of k_{obs} versus the concentration of Mn^{2+}−oxalate was hyperbolic (Figure 3), suggesting a binding interaction between the reactants leading to the oxidation of Mn^{2+} by LiPH2-compound II (LiP II). This two-step pathway can be described according to the equation:

$$\text{LiP II} + Mn^{2+}\text{−L} \overset{K_d}{\rightleftharpoons} \text{LiP II...}Mn^{2+}\text{−L} \xrightarrow{k} \text{LiP} + Mn^{3+}\text{−L} \quad (1)$$

where L is the ligand (oxalate), K_d is a dissociation constant (molar), and k is a first-order rate constant (s^{-1}). Assuming a rapid equilibrium for the binding of Mn^{2+} to LiP-compound II, the rate of Mn^{2+} oxidation can be given by eq 2.

$$k_{obs} = \frac{k}{1 + K_d/[Mn^{2+}\text{−oxalate}]} \quad (2)$$

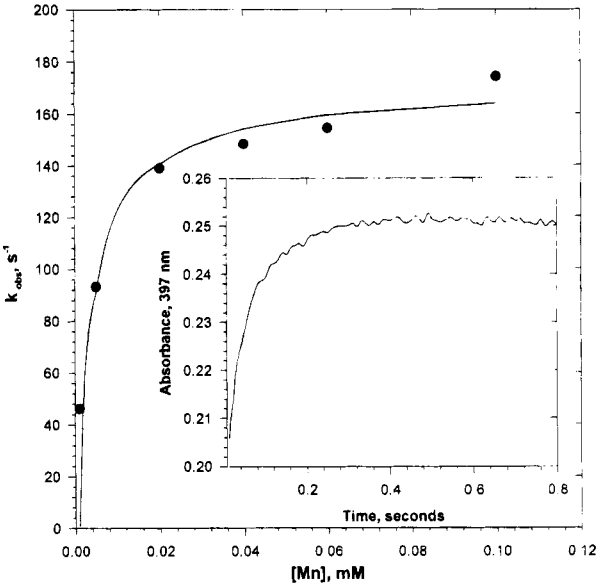

FIGURE 3: Reduction of lignin peroxidase compound II to the ferric enzyme by Mn^{2+}−oxalate. Compound II was formed by reacting compound I with 1 equiv of ferrocyanide. Compound I was formed as described for Figure 1. Typical incubations contained 1 μM LiPH2, 1 μM H_2O_2, 1 μM ferrocyanide, 500 μM oxalate and varying concentrations of Mn^{2+}. The k_{obs} values were obtained as described in Figure 1. The inset shows the actual stopped-flow trace for the increase in absorbance at 397 nm, corresponding to reduction of compound II to ferric enzyme by 60 μM Mn^{2+}−oxalate.

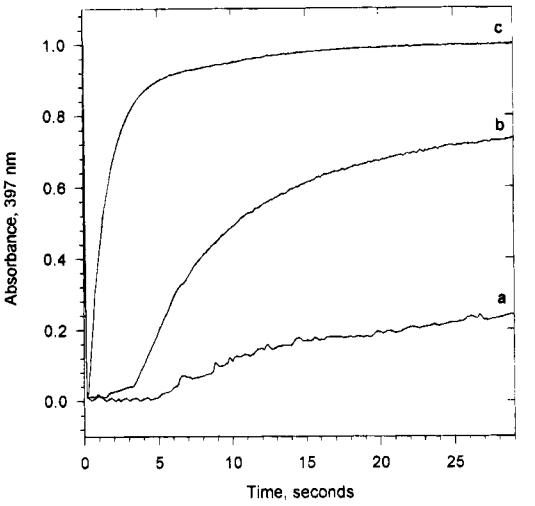

FIGURE 4: Absorbance of LiPH2 at 397 nm during catalysis in the presence and absence of Mn^{2+}. Trace a was obtained with 1 μM LiPH2, 50 μM H_2O_2 in 20 mM succinate buffer, pH 4.5. Trace b: same as in trace a but with 100 μM Mn^{2+}. Trace c: same as in trace b but with 500 μM oxalate.

The k_{obs} curve (Figure 3) for the reduction of LiPH2-compound II by Mn^{2+}−oxalate is best fit according to eq 2 with $K_d = (1.5 \pm 0.3) \times 10^{-5}$ M and $k = 215 \pm 6$ s^{-1}. Compound II formed by reduction of compound I with either Mn^{2+} or ferrocyanide yielded identical results.

Multiple Turnover Experiments. The 397 nm absorbance of LiPH2 in the presence of 50 equiv of H_2O_2 and excess Mn^{2+} is shown in Figure 4. At 397 nm, the isosbestic point for compounds I and II, the ferric enzyme exhibits an increase in absorbance. In the presence of excess H_2O_2 and Mn^{2+}, the enzyme undergoes multiple turnovers during which the steady-state intermediate is compound II. The enzyme returns to the ferric state as H_2O_2 is depleted. Thus, with

limiting H_2O_2 the return of the enzyme to the ferric state, observed at 397 nm, is a measure of the rate of catalysis. As shown in Figure 4 (trace a), in the absence of Mn^{2+}, the enzyme did not return to the ferric state during the course of the experiment. The slight increase in absorbance may be due to compound III formation (Renganathan & Gold, 1990). This was confirmed by the absorption spectrum of the enzyme (data not shown). When Mn^{2+} was included (trace b), the increase in 397 nm absorbance was slow, and only 60% of the enzyme returned to the ferric state. The loss of enzyme was probably due to the fact that succinate is a poor chelator for Mn^{2+} and unchelated Mn^{2+} cannot reduce compound II to ferric enzyme. If the rate of reduction of compound II is slow, H_2O_2 may react with compound II, forming compound III. Formation of compound III in the presence of H_2O_2 could result in a heme bleaching reaction (Wariishi & Gold, 1990; Jenzer et al., 1987). When 0.5 mM oxalate was included in the reaction mixture with Mn^{2+} (trace c), the rate of return of the enzyme to the ferric state was rapid. The final absorbance of the ferric enzyme corresponded well (98%) with the starting concentration of the enzyme. This suggests that Mn(II)−oxalate acts as a reductant for LiPH2, allowing for the complete turnover of the enzyme, and hence all of the enzyme returns to the ferric state.

Steady-State Kinetic Studies. Lignin peroxidase-catalyzed Mn^{3+} formation was followed at 270 nm in the presence of oxalate. The Mn^{3+}−oxalate complex exhibits an absorption maximum at 270 nm with an extinction coefficient of 5500 M^{-1} cm^{-1} (Kuan et al., 1993). The oxidation of Mn^{2+} by LiPH2 exhibited typical Michaelis−Menten kinetics (data not shown). The pH optimum for Mn^{2+}−oxalate oxidation by LiPH2 was found to be 4.5. The K_m's of LiPH2 for Mn^{2+}−oxalate and H_2O_2 were 19 μM and 42 μM, respectively. The maximal turnover rate of LiPH2 in the presence of Mn^{2+}−oxalate calculated from the double-reciprocal plot was 202 s^{-1}. The apparent second-order rate constant ($k_{cat}/K_m = 1 \times 10^7$ M^{-1} s^{-1}) for the reaction of the Mn^{2+}−oxalate complex with LiPH2 is in close agreement (within experimental error) with the second-order rate constant (8×10^6 M^{-1} s^{-1}) obtained from transient state kinetics.

ESR Experiments. Divalent manganese is paramagnetic with a spin quantum number of $^5/_2$ and therefore exhibits an ESR signal. On the other hand, Mn^{3+} is ESR-silent. Hence, the oxidation of Mn^{2+} can be followed as a decrease in ESR signal intensity. The ESR spectrum of 100 μM Mn^{2+} is shown in Figure 5 (trace A). The ESR spectrum taken in a reaction mixture containing LiPH2, Mn^{2+}, and H_2O_2 is shown as trace B. The decrease in signal intensity (Figure 5, trace B) corresponded with an increase in absorbance at 270 nm (data not shown) that was sensitive to dithionite. The decrease in signal intensity was more with VA in the reaction mixture (trace C). A similar decrease was observed when oxalate was included in the reaction mixture (trace E). With VA in the reaction mixture, SOD inhibited the disappearance of Mn^{2+} (trace D), but with oxalate, SOD had no effect, and neither did VA (traces F and G).

Oxygen Evolution Experiments. Aitken and Irvine (1990) have shown that Mn^{3+} reacts with H_2O_2, leading to O_2 production. Hence, Mn^{3+} formation can also be followed by measuring the evolved O_2 in a system containing H_2O_2 and generating Mn^{3+}. The O_2 evolved in reaction mixtures with Mn^{2+}, LiPH2, and H_2O_2 with or without VA (traces A and B, respectively) is shown in Figure 6. When Mn^{2+} was omitted from the reaction mixture, O_2 production was not observed (trace C). To confirm whether the oxygen production was due to the reaction of Mn^{3+} with H_2O_2, Mn^{3+}−acetate was reacted with H_2O_2 (trace D). The extent of oxygen evolution was directly proportional to H_2O_2 concentration (Figure 7), and showed a hyperbolic concentration dependence with increasing [manganese] (inset).

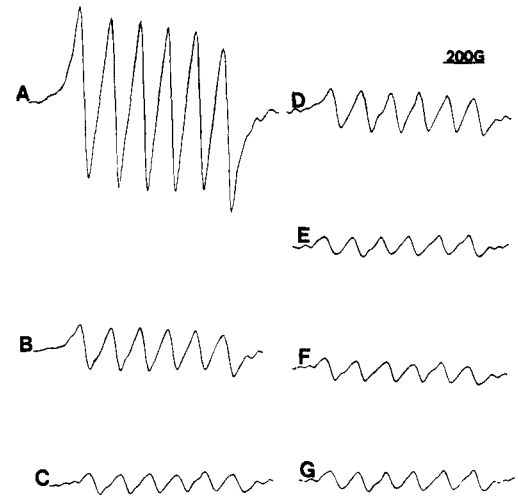

FIGURE 5: Electron spin resonance spectra of Mn^{2+}. Spectrum A was obtained with 100 μM Mn^{2+} in 20 mM succinate buffer, pH 4.5. Spectrum B was obtained with 100 μM Mn^{2+}, 0.6 μM LiPH2, and 100 μM H_2O_2 in 20 mM succinate buffer, pH 4.5. Spectrum C: same as for spectrum B but with 2 mM VA. Spectrum D: same as for spectrum C but with 20 units/mL SOD. Spectrum E: same as for spectrum B but with 500 μM oxalate. Spectrum F: same as for spectrum E but with 2 mM VA. Spectrum G: same as for spectrum E but with 20 units/mL SOD. Spectrometer settings were 50 kHz modulation frequency, 1.0 G modulation amplitude, 20 mW microwave power, 100 G sweep width, and a gain of 1×10^4. All spectra were recorded 30 s after initiation of the reaction with H_2O_2.

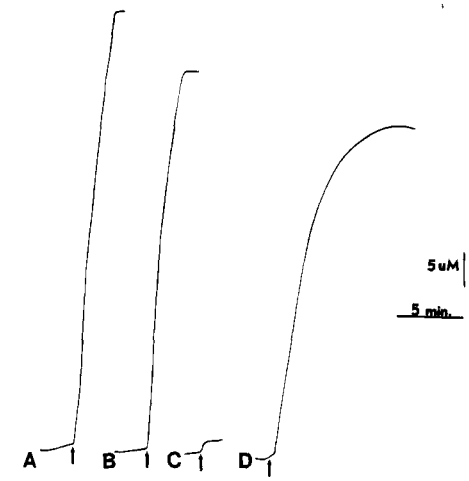

FIGURE 6: Oxygen production catalyzed by LiPH2 during oxidation of Mn^{2+} and VA. Trace A was obtained with 0.38 μM LiPH2, 500 μM H_2O_2, 100 μM Mn^{2+}, and 2 mM VA in pH 4.5 succinate buffer (20 mM). Trace B: same as trace A except VA was omitted. Trace C: same as trace A except Mn^{2+} was omitted. Trace D was obtained with 100 μM Mn^{3+} and 500 μM H_2O_2 in 20 mM succinate buffer, pH 4.5. The arrows indicate the addition of H_2O_2.

Inhibition of Veratryl Alcohol Oxidation. To confirm that the oxidation of the manganese was not due to any contamination by a manganese-dependent peroxidase, the inhibition of VA oxidase activity of LiPH2 by Mn^{2+} was studied by monitoring the formation of veratryl aldehyde at

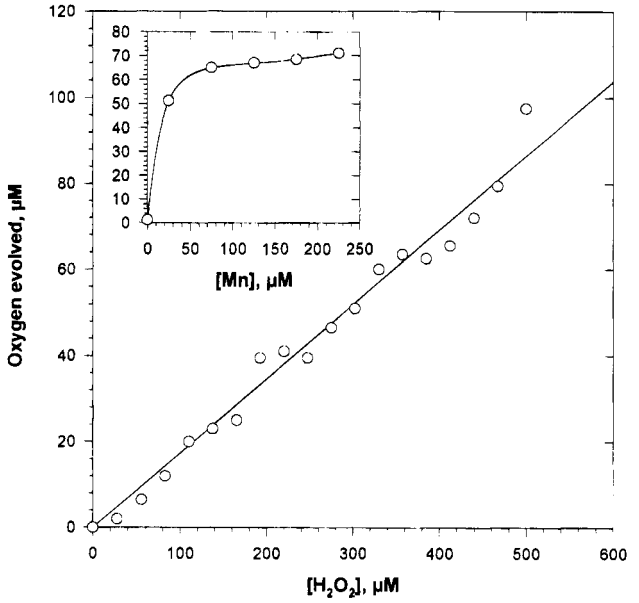

FIGURE 7: Effect of H_2O_2 on oxygen evolution during Mn^{2+} oxidation by LiPH2. Reaction mixtures contained 0.38 μM LiPH2, 100 μM Mn^{2+}, and 500 μM oxalate in pH 4.5 succinate buffer and varying amounts of H_2O_2. The inset shows the effect of Mn^{2+} on LiPH2-catalyzed oxygen production. The reaction conditions were the same as described above except that H_2O_2 concentration was kept constant and [Mn^{2+}] was varied.

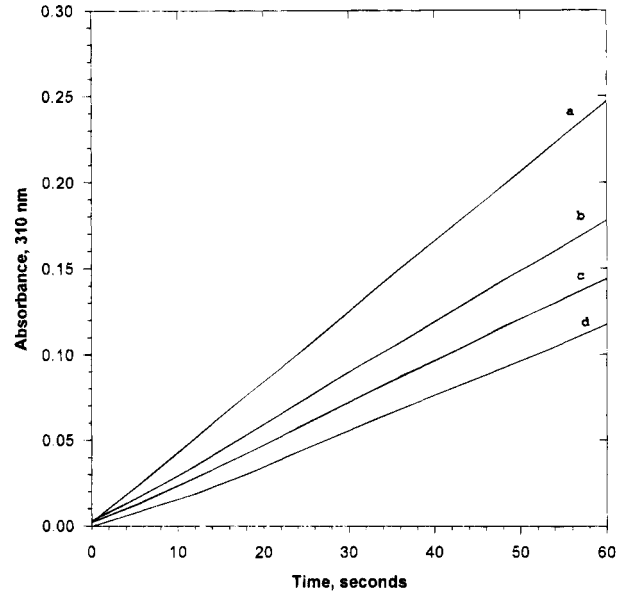

FIGURE 8: Inhibition of VA oxidase activity of LiPH2 by Mn^{2+}. Reaction mixtures contained 0.06 μM LiPH2, 100 μM H_2O_2, 2 mM VA, 500 μM oxalate, in 20 mM succinate buffer, pH 4.5, and varying concentrations of Mn^{2+}: (a) no Mn^{2+}; (b) 10 μM Mn^{2+}; (c) 20 μM Mn^{2+}; (d) 30 μM Mn^{2+}.

310 nm (Figure 8). The rationale for this experiment was that if Mn^{2+} is a substrate for LiPH2 it should inhibit VA oxidation by LiPH2. Moreover, since manganese-dependent peroxidases cannot oxidize VA, any contaminating enzyme should not interfere in this activity. Veratryl alcohol oxidation by LiPH2 was inhibited by Mn^{2+} in a reaction mixture containing 0.06 μM LiPH2, 2 mM VA, 500 μM oxalate, and 100 μM H_2O_2. The K_i for Mn^{2+}–oxalate inhibition of VA oxidation by LiPH2 was calculated to be 20 μM.

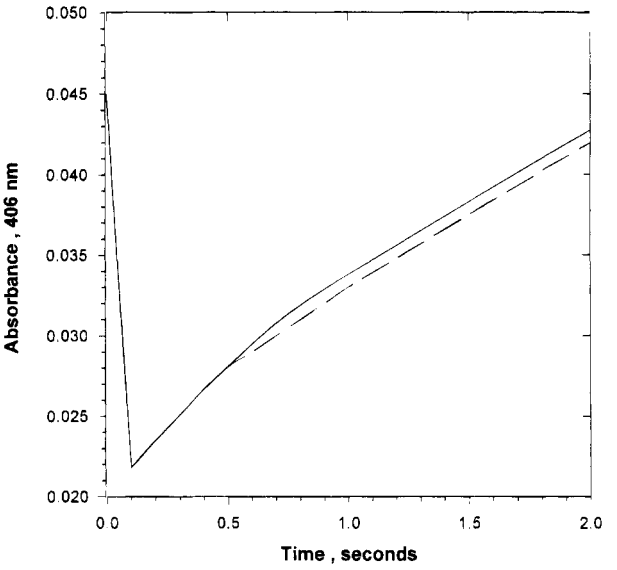

FIGURE 9: Simulation of steady-state turnover kinetics using rate constants obtained from transient state kinetics. The solid line is the 406 nm absorbance during steady-state turnover of LiPH2 (1 μM) in the presence of 50 μM H_2O_2, 100 μM Mn^{2+}, and 500 μM oxalate in 20 mM succinate buffer, pH 4.5. The dashed line (– –) shows the data obtained by simulation. This was simulated using the mechanism shown in Figure 10 and the rate constants given in the legend to that figure.

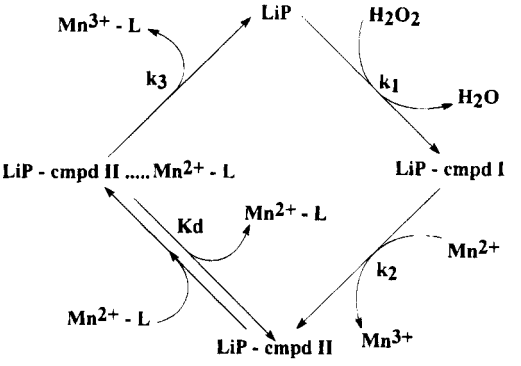

FIGURE 10: Mechanism for Mn^{2+} oxidation by LiPH2 compounds and II. This mechanism was used to simulate the data in Figure 9. The rate constants used in the simulation are $k_1 = 2 \times 10^6$ M^{-1} s^{-1}, $k_2 = 8 \times 10^7$ M^{-1} s^{-1}, $K_d = 1.52 \times 10^{-5}$ M, and $k_3 = 215$ s^{-1}.

Simulation of Steady-State Turnover. Transient-state kinetic data and the proposed mechanism can be validated by simulation of steady-state turnover with the rate constants obtained from pre-steady-state conditions. This serves to verify whether a set of rate constants are consistent with the observed data. The 406 nm absorbance of LiPH2 during catalysis in the presence of Mn^{2+} and oxalate is shown in Figure 9. The experimental conditions were the same as described for multiple turnover experiments (Figure 4) except that the heme absorbance was followed at 406 nm. The dashed line was obtained by simulation of the mechanism shown in Figure 10. The rate constants used are shown in that figure legend. Simulation demonstrated that the rate constants obtained in the present study can readily account for the steady-state turnover of lignin peroxidase in the presence of H_2O_2 and Mn^{2+}–oxalate at pH 4.5.

DISCUSSION

The ability of manganese-dependent peroxidases to oxidize Mn^{2+} has been well established (Wariishi et al., 1989; Glenn

et al., 1986). Popp et al. (1990) reported that a lignin peroxidase could oxidize Mn^{2+}, but they proposed a free radical mechanism where VA and oxalate are involved and oxidation is indirect. We demonstrate here that Mn^{2+} is directly oxidized by lignin peroxidases. We further show that oxalate chelation facilitates the reaction of Mn^{2+} with compound II, as has been shown for manganese-dependent peroxidases (Kuan et al., 1993). We also show that at pH 4.5, the physiological pH of the fungus, the k_{cat} for LiPH2 oxidation of Mn^{2+} is 202 s^{-1}, 25 times the k_{cat} for oxidation of VA (8 s^{-1}; Tuisel et al., 1990). These findings would suggest that an important role of LiPH2 is to oxidize Mn^{2+}. At pH 4.5, the rate of reaction of Mn^{2+}, chelated or free, with compound I was estimated to be near 10^8 M^{-1} s^{-1}, too fast to monitor using stopped-flow techniques. A rate constant of 4.2×10^4 M^{-1} s^{-1} was obtained at pH 6.0. Similar results were obtained at pH 3.0, suggesting that the pH optimum for the reaction lies somewhere between these values. Compound II only oxidized chelated manganese with the optimum activity at pH 4.5. We investigated oxalate as a Mn^{2+} chelator capable of supporting steady-state turnover of the enzyme since oxalate is synthesized and excreted by *P. chrysosporium* (Kuan & Tien, 1993; Barr et al., 1992). The K_d for binding of Mn^{2+}−oxalate to compound II was found to be $(1.5 \pm 0.3) \times 10^{-5}$ M, and a first-order rate constant for the reaction of Mn^{2+}−oxalate with compound II was calculated to be 215 ± 6 s^{-1}. This is fast enough to account for the steady-state turnover of the enzyme, with the k_{cat} of 202 s^{-1}. Since there are two Mn^{3+} formed per turnover of the enzyme (Wariishi et al., 1992), the k_{cat} should theoretically be 430 s^{-1} (215 $s^{-1} \times 2$). The low k_{cat} may be explained by the reaction of Mn^{3+} with H_2O_2 leading to O_2 production. This oxygen evolution is directly proportional to H_2O_2 concentration (Figure 7). Hence, above 50 μM H_2O_2, Mn^{3+} formation is inhibited (50% at 100 μM H_2O_2). Furthermore, the steady-state kinetic analyses were performed with 50 μM H_2O_2 (K_m = 42 μM), which would mean that the enzyme turnover rate would be approximately half the maximal. If the V_{max} is indeed 2× the velocity obtained at about 50 μM H_2O_2, then the k_{cat} at saturated H_2O_2 would be 404 s^{-1}, which agrees closely with the theoretical value of 430 s^{-1}.

The K_m of LiPH2 for Mn^{2+}−oxalate was also obtained by steady-state studies. A value of 19 μM was obtained, which is close to that reported for manganese-dependent peroxidases (13 μM), suggesting that these enzymes are very close in their ability to oxidize Mn^{2+}.

It may be argued that the steady-state oxidation of Mn^{2+} could occur if the LiPH2 preparation was contaminated with a manganese-dependent peroxidase. This would require that under multiple turnover conditions only manganese-dependent peroxidase would be operative. Conversely, the LiPH2 present would be unable to turn over and be converted to compound II or III (Renganathan & Gold, 1990). This was not observed as in the presence of Mn^{2+}−oxalate all of the enzyme included in the reaction returned to the ferric state after depletion of H_2O_2 (Figure 4). This indicated that Mn^{2+}−oxalate can act as a reductant for both compounds I and II of LiPH2. This same experiment also demonstrated that in the absence of Mn^{2+} the enzyme did not return to the ferric state but instead was converted to compound III, as confirmed by the absorption spectrum.

To further confirm that LiPH2 was oxidizing Mn^{2+}, inhibition of VA oxidation was studied. At concentrations as low as 10 μM Mn^{2+}, VA (2 mM) oxidation by LiPH2 was inhibited. This is consistent with the finding that LiPH2 has a low K_m for Mn^{2+}−oxalate. Furthermore, the observed inhibition constant (K_i = 20 μM) is in close agreement with the K_m, as would be expected if Mn^{2+}−oxalate is an alternate substrate for LiPH2 (Segel, 1975). These results are in contrast to an earlier published report that Mn^{2+} is not a substrate for lignin peroxidases (Popp et al., 1990). It is possible that these differences are attributed to different isozymes used in the two studies [i.e., the isozyme used by Popp et al. (1990) was LiP H6]. However, they also reported, but did not explain, the Mn^{2+}-dependent inhibition of VA oxidation by lignin peroxidase isozyme H6. The findings in this study can readily explain these results. Interestingly, we have also observed that the VA oxidase activity of all lignin peroxidase isozymes is inhibited by Mn^{2+}, though to varying extents (manuscript in preparation).

Furthermore, the free radical mechanism proposed earlier (Popp et al., 1990), where oxalate oxidation by the VA cation radical results in the formation of $CO_2^{\bullet-}$, which then reduces O_2 to $O_2^{\bullet-}$, which then oxidizes Mn^{2+}, suggests that increasing oxalate concentration would increase the rate of Mn^{2+} oxidation. This was not observed as their data (Popp et al., 1990) showed that increasing oxalate concentration inhibited the oxidation of Mn^{2+}. Their results, however, can readily be explained if lignin peroxidase directly oxidizes Mn^{2+}−oxalate. Under the concentrations of oxalate (10 mM) and Mn^{2+} (1 mM) used by these investigators, a significant fraction of manganese (65%) will be chelated by two oxalate ligands, preventing it from approaching the active site, resulting in inhibition of Mn^{3+} formation (Kuan et al., 1993). Furthermore, under our experimental conditions we observed that Mn(III) reacts with H_2O_2 to form O_2; hence, the reverse reaction ($O_2^{\bullet-} + Mn^{2+} + 2H^+ \rightarrow Mn^{3+} + H_2O_2$) would not be favorable (Archibald & Fridovich, 1982; Cabelli & Bielski, 1984; Bielski et al., 1984). Also, Cabelli et al. (1984) and Bielski et al. (1984) have shown that oxidation of Mn^{2+} by $O_2^{\bullet-}$ is favorable only in the presence of ligands that stabilize Mn(III). Oxalate decarboxylation by Mn(III) is well-known (Khindaria et al., 1994; Jones et al., 1961). Hence, it does not stabilize Mn(III), eliminating the possibility for the reaction proposed by Popp et al. (1990).

Direct oxidation of Mn^{2+} by LiPH2 is also supported by the results of ESR studies. In the absence of VA, oxalate, or molecular oxygen, Mn^{2+} was oxidized as evident from the reduced ESR signal intensity. The addition of VA further decreased the signal intensity, suggesting increased formation of Mn^{3+}. This can be explained by considering that in the absence of a chelator Mn^{2+} does not react with compound II; hence, VA completes the catalytic cycle, allowing for continued turnover of the enzyme. Superoxide dismutase did inhibit manganese oxidation about 5%, but this is not consistent with the earlier conclusion that $O_2^{\bullet-}$ is primarily responsible for Mn^{2+} oxidation (Popp et al., 1990). Furthermore, in the presence of oxalate as a chelator, neither VA nor SOD had any effect on the oxidation of Mn^{2+}. These results support our hypothesis that Mn^{2+} is primarily oxidized directly by the enzyme and are consistent with proposing a mechanism for direct oxidation of Mn^{2+}−oxalate by LiPH2 (Figure 10).

The conclusions are also supported by the confirmation of the steady-state results by kinetic simulation using the rate constants obtained from transient state kinetics. This is especially significant since we have observed that Mn(III) can oxidatively revert LiP-compound III back to ferric enzyme, thus preventing permanent inactivation (unpublished data). It is also known that Mn(III) can react with H_2O_2, which would reduce H_2O_2 levels sufficiently to mitigate the inactivation of the enzyme (Aitken & Irvine, 1990). The faster rate of oxidation of Mn(II) (than VA) would suggest that Mn(III) may act as a better mediator for indirect oxidations.

In conclusion, we have shown that Mn^{2+} is directly oxidized by lignin peroxidases and that the free radical mediated oxidation of manganese (i.e., by $O_2^{\bullet-}$) may account for up to only 5% of all manganese oxidized by the enzyme. Furthermore, the manganese peroxidase assays of crude peroxidase preparations may be erroneous, as lignin peroxidase may contribute the major share of this activity. Also, the concentration of H_2O_2 used in the manganese peroxidase assay will greatly affect the observed activity due to the reaction of Mn^{3+} with H_2O_2. In the future, we would like to further determine the factors responsible for varying amounts of Mn^{2+} oxidase activity of different lignin peroxidase isozymes.

ACKNOWLEDGMENT

We express our sincere gratitude to Terri Maughan for help in preparing the manuscript. We thank Yixin Ben for the production of the enzyme, John Brollini for help with the experiments, and Jeffery Guo for technical advice.

REFERENCES

Aitken, M. D., & Irvine R. L. (1990) *Arch. Biochm. Biophys. 276*, 405−414.

Archibald, F. S., & Fridovich. I. (1982) *Arch. Biochem. Biophys. 214*, 452−463.

Barr, D. P., & Aust, S. D. (1994) *Environ. Sci. Technol. 28*, 78A-87A.

Barr, D. P., Shah, M. M., Grover, T. A., & Aust, S. D. (1992) *Arch. Biochem. Biophys. 279*, 158−166.

Barshop, B. A., Wrenn, R. F., & Frieden, C. (1983) *Anal. Biochem. 130*, 134−145.

Bielski, B. H. J., Arudi, R. L., & Cabelli, D. E. (1984) in *Oxygen Radicals in Chemistry and Biology* (Bors, W., Saran, M., & Tait, D., Eds.) pp 1−15, Walter de Gruyter, Berlin.

Cabelli, D. E., & Bielski, B. H. J. (1984) *J. Phys. Chem. 88*, 3111−3115.

Cui, F., & Dolphin, D. (1990) *Holzforschung 44*, 279−283.

Farrell, R. L., Murtagh, K. E., Tien, M., Mozuch, M. D., & Kirk, T. K. (1989) *Enzyme Microb. Technol. 11*, 322−328.

Glenn, J. K., Akileswaran, L., & Gold, M. H. (1986) *Arch. Biochem. Biophys. 251*, 688−696.

Khindaria, A., Grover, T. A., & Aust, S. D. (1994) *Arch. Biochem. Biophys. 314*, 301−306.

Kirk, T. K., & Farrell, R. L. (1987) *Annu. Rev. Microbiol. 41*, 465−505.

Kuan, I., & Tien, M. (1993) *Proc. Natl. Acad. Sci. U.S.A. 90*, 1242−1246.

Kuan, I., Johnson, K. A., & Tien M. (1993) *J. Biol. Chem. 268*, 20064−20070.

Popp, J. L., Kalyanaraman, B., & Kirk, T. K. (1990) *Biochemistry 29*, 10475−10480.

Renganathan, V., & Gold, M. H. (1990) *J. Biol. Chem. 265*, 2070−2077.

Segel, I. H. (1975) in *Enyzme Kinetics* (Segel, I. H., Ed.) pp 274−344, John Wiley & Sons, Inc., New York.

Tien, M. (1987) *CRC Crit. Rev. Microbiol. 15*, 141−168.

Tuisel, H., Sinclair, R., Bumpus, J. A., Ashbaugh, W., Brock, B. J., & Aust, S. D. (1990) *Arch. Biochem. Biophys. 279*, 158−166.

Wariishi, H., Dunford, H. B., MacDonald, I. D., & Gold, M. H. (1986) *J. Biol. Chem. 264*, 3335−3340.

Wariishi, H., Valli, K., & Gold, M. H. (1992) *J. Biol. Chem. 267*, 23688−23695.

Young, H. E., & Guinn, V. P. (1966) *TAPPI J. 49*, 190−197.

BI943003V